

Pseudogap in the normal state of superfluid condensate formed by ultracold Fermi gases with particle-hole fluctuation

Xiao-Xia Ruan(阮小霞), Yu-Qi Wang(王钰淇), Si-Ying Chen(陈思颖), Xiao-Bin Hua(花晓彬), Hao Gong(宫昊)
Citation: Chin. Phys. B. 35, 090307 (2026). DOI: 10.1088/1674-1056/ae41a0 | CSTR: 32038.14.CPB.ae41a0
http://cpb.iphy.ac.cn; http://iopscience.iop.org/cpb

What follows is a list of articles you may be interested in

Three-party quantum key agreement with seven-particle entangled states against collective noise: IBM Qiskit implementation

She-Xiang Jiang(蒋社想), Jin-Huan Li(李金欢)
Chin. Phys. B. 35, 070307 (2026). DOI: 10.1088/1674-1056/ae53b6 | CSTR: 32038.14.CPB.ae53b6

Ultracold atomic absorption imaging system in high magnetic fields

Yuying Chen(陈玉莹), Zhengxi Zhang(张正熙), Hongmian Shui(税鸿冕), Yun Liang(梁芸), Fansu Wei(魏凡粟), Xiaoji Zhou(周小计)
Chin. Phys. B. 34, 053303 (2025). DOI: 10.1088/1674-1056/adc7f6 | CSTR: 32038.14.CPB.adc7f6

Single-scattering characteristics of melting ice crystal particles in the millimeter-wave band

Xue-Hai Zhang(张学海), Wen-Bo Liu(刘文博), Xin-Hui Zhang(张欣慧), He-Li Wei(魏合理), Wei-Dong Li(李卫东), Jin-Long Duan(段金龙), Shu-Guang Zou(邹曙光), Jia Liu(刘佳), Cong-Ming Dai(戴聪明)
Chin. Phys. B. 34, 050307 (2025). DOI: 10.1088/1674-1056/adbd23 | CSTR: 32038.14.CPB.adbd23

Interference-induced suppression of particle emission from a Bose–Einstein condensate in lattice with time-periodic modulations

Long-Quan Lai(赖龙泉), Zhao Li(李照)
Chin. Phys. B. 33, 100303 (2024). DOI: 10.1088/1674-1056/ad607b

Topological superfluid in a two-dimensional polarized Fermi gas with spin-orbit coupling and adiabatic rotation

Lei Qiao(乔雷), Cheng Chi(迟诚)
Chin. Phys. B. 26, 120304 (2017). DOI: 10.1088/1674-1056/26/12/120304

Pseudogap in the normal state of superfluid condensate formed by ultracold Fermi gases with particle–hole fluctuation

Xiao-Xia Ruan(阮小霞)[1,2,†], Yu-Qi Wang(王钰淇)[1], Si-Ying Chen(陈思颖)[1], Xiao-Bin Hua(花晓彬)[1], and Hao Gong(宫昊)[3,‡]

[1] *School of Physics and Electronic Engineering, Jiangsu University, Zhenjiang* 212013, *China*
[2] *National Laboratory of Solid State Microstructures, Nanjing University, Nanjing* 210093, *China*
[3] *Faculty of Science, Bengbu University, Bengbu* 233030, *China*

(Received 2 September 2025; revised manuscript received 29 January 2026; accepted manuscript online 4 February 2026)

In the normal state of a superfluid condensate, like the Bardeen–Cooper–Schrieffer (BCS) superconducting state, we do not expect a gapped feature in the single-particle spectral function. Here we calculate the spectral function and single-particle density of states (DOS) of ultracold Fermi gases at different temperatures in the normal state. The calculation is conducted based on the non-self-consistent T-matrix approximation (nTMA) with particle–hole fluctuation. It is found that a dip structure emerges in the DOS above the superfluid phase-transition temperature T_c. We attribute this dip structure to the pseudogap, and its temperature is determined. From the temperature dependence of the spectral function, we also find another characteristic temperature where a two-peak structure disappears. The results provide deep insight into the superfluid condensate formed by ultracold fermions.

Keywords: Bardeen–Cooper–Schrieffer (BCS), pseudogap, particle–hole fluctuation

PACS: 03.75.Ss, 05.30.Fk, 03.75.Hh

DOI: 10.1088/1674-1056/ae41a0 **CSTR:** 32038.14.CPB.ae41a0

1. Introduction

In recent years, the degenerate atomic gases have attracted broad interest both experimentally and theoretically.[1–4] The ultracold Fermi gases provide an ideal platform for the study of strongly interacting systems such as high-T_c superconductors and neutron stars because of the clean and well-controlled environment.[5] The crossover from Bardeen–Cooper–Schrieffer (BCS) superfluidity to Bose–Einstein condensation (BEC) can be achieved in ultracold Fermi gases by the accurate control of interaction via Feshbach resonance. The interaction strength can be described by the parameter $(k_F a_s)^{-1}$, where k_F is the Fermi wave vector and a_s is the s-wave scattering length. At the resonance, the system is the so-called unitary limit. The BCS side corresponds to $(k_F a_s)^{-1} < 0$, and the BEC side corresponds to $(k_F a_s)^{-1} > 0$.

Pseudogap is an important phenomenon in high-T_c superconductors.[6,7] Recently, a pseudogap phenomenon was observed in the Fe-based superconductor $KCa_2Fe_4As_4F_2$ through the measurement of optical properties.[8] The origin of the pseudogap is widely debated. Different views such as preformed pairs,[9–14] antiferromagnetic spin fluctuations,[15,16] and a hidden order[17] have been proposed. High-temperature superconductivity systems are complex, and it is hoped that the study of the simpler systems of ultracold Fermi gases will contribute to the understanding of the pseudogap phenomenon in high-T_c superconductors. Reference [18] reported the observation of a pair-fluctuation-driven pseudogap in homogeneous unitary Fermi gases by precisely measuring the fermion spectral function via momentum-resolved microwave spectroscopy with a negligible final-state effect. In this paper, we investigate the pseudogap temperature in ultracold Fermi gases. There are two criteria for the pseudogap. The first is that a pseudogap refers to a depression in the DOS around the Fermi level for temperatures above T_c. In this paper, we employ this definition to calculate the pseudogap temperature T^* below which a dip structure appears in the DOS in the normal state. The second is the existence of a pseudogap associated with the appearance of double-peak structure in the spectral function $A(\boldsymbol{k}, \omega)$ as a function of ω at $k = k_F$. We calculate another pseudogap temperature T^{**} where a two-peak structure disappears in the spectral weight $A(\boldsymbol{k}, \omega)$ in the normal state.

Pairing fluctuation plays a key role in the calculation of DOS. There are two kinds of fluctuation. One is the fluctuation from the particle–particle channel discussed by Nozières and Schmitt–Rink (NSR)[19], and the other is the particle–hole fluctuation pointed out by Gorkov and Melik–Barkhudarov (GMB)[20] at first. Reference [21] pointed out that when the system moved from the BCS side toward the BEC side, the GMB fluctuation became weaker and the NSR fluctuation became stronger. Taking into account the effect of particle–hole fluctuation, we calculate the spectral function and hence DOS

†Corresponding author. E-mail: rxxlu@ujs.edu.cn
‡Corresponding author. E-mail: gh@bbc.edu.cn

© 2026 Chinese Physical Society and IOP Publishing Ltd. All rights, including for text and data mining, AI training, and similar technologies, are reserved.

within the framework of the non-self-consistent T-matrix approach. In addition to the nTMA approximation, there are another two T-matrix approaches. They are the $(GG)G$ approximation investigated by Haussmann[22–24] and the $(GG_0)G_0$ approximation used by Levin's group[25] with an asymmetric form for the pair propagator. From the behavior of the spectral function and DOS, we obtain two pseudogap temperatures. We also compare our results with the theoretical results without the GMB approximation[26] and the experimental results.[18]

This paper is organized as follows. In Section 2, we recall the GMB approximation, also called induced interaction, the spectral function and DOS. In Section 3, we report our numerical results of the spectral function, DOS and pseudogap temperature. The comparisons of our obtained pseudogap temperatures with the theoretical predictions without particle–hole fluctuation and the experimental data are also given in this section. Section 4 gives a summary. Throughout this paper, we take $\hbar = k_{\rm B} = 1$.

2. Induced interaction and DOS

In this paper, a homogeneous two-component Fermi gas labelled by pseudospin $\sigma = \uparrow, \downarrow$ is considered. For a broad Feshbach resonance, one can employ a single-channel model and the system is described by the Hamiltonian

$$\begin{aligned} &H - \mu N \\ &= \sum_{\boldsymbol{k},\sigma} \xi_{\boldsymbol{k}} c^{\dagger}_{\boldsymbol{k}\sigma} c_{\boldsymbol{k}\sigma} - U \sum_{\boldsymbol{q}\boldsymbol{k}\boldsymbol{k}'} c^{\dagger}_{\boldsymbol{k}+\boldsymbol{q}/2\uparrow} c^{\dagger}_{-\boldsymbol{k}+\boldsymbol{q}/2\downarrow} c_{-\boldsymbol{k}'+\boldsymbol{q}/2\downarrow} c_{\boldsymbol{k}'+\boldsymbol{q}/2\uparrow}. \end{aligned} \tag{1}$$

Here, $c_{\boldsymbol{k}\sigma}$ is the annihilation operator for a Fermi atom with momentum $\boldsymbol{k}$ and pseudospin σ. $\xi_{\boldsymbol{k}} = \varepsilon_{\boldsymbol{k}} - \mu$ is the kinetic energy, which is measured from the chemical potential μ. The pairing interaction $-U$ is a tunable parameter through Feshbach resonance. We relate it to the s-wave scattering length $a_{\rm s}$ via

$$\frac{1}{-U} = \frac{m}{4\pi a_{\rm s}} - \sum_{\boldsymbol{k}} \frac{1}{2\varepsilon_{\boldsymbol{k}}}. \tag{2}$$

2.1. Induced interaction

Following the method used in Ref. [21], with the inclusion of the particle–hole fluctuation, the effective interaction is

$$-U_{\rm eff} = \frac{-U}{1 - U\langle\chi\rangle}. \tag{3}$$

Here, $\langle\chi\rangle$ is the average of the polarization function χ, which is a function of the transferred momentum and the frequency.

The entanglement between pairing and screening was taken into account in the calculation of the GMB contribution throughout the BCS–BEC crossover in Refs. [27–29]. For simplicity, we ignore the entanglement. This simplification is qualitatively valid, as pointed out in Ref. [30]. The effect of induced interaction is treated by an averaging procedure over the Fermi surface. In Ref. [21], $\langle\chi\rangle$ was obtained by setting the frequencies and total momentum to zero, taking all the initial and final states of atoms from the Fermi surface and then averaging over scattering angles. We borrow the average of χ from Ref. [21] directly. $\mu > 0$, the average of χ is

$$\langle\chi\rangle = \frac{m}{4\pi^2} \int_{-1}^{1} {\rm d}\cos\theta \int_0^{\infty} {\rm d}k \frac{k}{k'} f_k \ln\left|\frac{k'-2k}{k'+2k}\right|. \tag{4}$$

Here, $k' = k_{\rm F}\sqrt{2(1+\cos\theta)}$, $k_{\rm F}$ is the Fermi wave vector, and $f_k = f(\xi_{\boldsymbol{k}})$ is the Fermi distribution function.

2.2. Spectral function and DOS

The single-particle dressed thermal Green's function is

$$\mathcal{G}_{\boldsymbol{k}}(\mathrm{i}\omega_n) = \frac{1}{\mathrm{i}\omega_n - \xi_{\boldsymbol{k}} - \Sigma(\boldsymbol{k}, \mathrm{i}\omega_n)}. \tag{5}$$

Here, ω_n is the fermion Matsubara frequency and $\Sigma(\boldsymbol{k}, \mathrm{i}\omega_n)$ is the self-energy correction.

The single-particle spectral function is determined by the imaginary part of the retarded Green's function via

$$A(\boldsymbol{k}, \omega) = -\frac{1}{\pi}{\rm Im}[\mathcal{G}(\boldsymbol{k}, \mathrm{i}\omega_n \to \omega + \mathrm{i}\delta)]. \tag{6}$$

In terms of the real part and the imaginary part of the retarded self-energy, $A(\boldsymbol{k}, \omega)$ can be expressed as

$$A(\boldsymbol{k}, \omega) = -\frac{1}{\pi} \frac{{\rm Im}\Sigma^{\rm R}(\boldsymbol{k}, \omega)}{[\omega - \xi_{\boldsymbol{k}} - {\rm Re}\Sigma^{\rm R}(\boldsymbol{k}, \omega)]^2 + [{\rm Im}\Sigma^{\rm R}(\boldsymbol{k}, \omega)]^2}. \tag{7}$$

The real part of the retarded self-energy ${\rm Re}\Sigma^{\rm R}(\boldsymbol{k}, \omega)$ can be obtained via the Kramers–Kronig relation. For calculating the spectral function, the imaginary part of the retarded self-energy is crucial. It can be obtained from the particle-particle scattering matrix via

$$\begin{aligned} {\rm Im}\Sigma^{\rm R}(\boldsymbol{k}, \omega) \;=\; & \sum_{\boldsymbol{q}} [b(\omega + \xi_{\boldsymbol{q}-\boldsymbol{k}}) + f(\xi_{\boldsymbol{q}-\boldsymbol{k}})] \\ & \times {\rm Im}[\Gamma^{\rm R}(\boldsymbol{q}, \omega + \xi_{\boldsymbol{q}-\boldsymbol{k}})], \end{aligned} \tag{8}$$

where $f(x) = 1/(\mathrm{e}^{\beta x} + 1)$ is the Fermi distribution function and $b(x) = 1/(\mathrm{e}^{\beta x} - 1)$ is the Bose distribution function. The expression of the particle–particle scattering matrix is

$$\begin{aligned} \Gamma(\boldsymbol{q}, \mathrm{i}\nu_n) \;&=\; \frac{-U_{\rm eff}}{1 - U_{\rm eff}\Pi(\boldsymbol{q}, \mathrm{i}\nu_n)} \\ &=\; \frac{1}{\dfrac{m}{4\pi a_{\rm s}} - \displaystyle\sum_{\boldsymbol{k}} \frac{1}{2\varepsilon_{\boldsymbol{k}}} + \langle\chi\rangle + \Pi(\boldsymbol{q}, \mathrm{i}\nu_n)}, \end{aligned} \tag{9}$$

where ν_n is the boson Matsubara frequency. The pair propagator $\Pi(\boldsymbol{q}, \mathrm{i}\nu_n)$ is given by

$$\Pi(\boldsymbol{q}, \mathrm{i}\nu_n) \;=\; T \sum_{\boldsymbol{k}, \omega_n} \mathcal{G}^0_{\boldsymbol{k}+\boldsymbol{q}/2}(\mathrm{i}\nu_n + \mathrm{i}\omega_n) \mathcal{G}^0_{-\boldsymbol{k}+\boldsymbol{q}/2}(-\mathrm{i}\omega_n)$$

$$= \sum_{\boldsymbol{k}} \frac{1 - f(\xi_{\boldsymbol{k}+\boldsymbol{q}/2}) - f(\xi_{\boldsymbol{k}-\boldsymbol{q}/2})}{\xi_{\boldsymbol{k}+\boldsymbol{q}/2} + \xi_{\boldsymbol{k}-\boldsymbol{q}/2} - \mathrm{i}\nu_n}. \tag{10}$$

The density of states $\rho(\omega)$ can be obtained by integrating the single-particle spectral function over momentum:[31–35]

$$\rho(\omega) = \int \frac{\mathrm{d}\boldsymbol{k}}{(2\pi)^3} A(\boldsymbol{k}, \omega). \tag{11}$$

3. Results

In the following, we present our results for the spectral function, DOS, and the pseudogap temperature with the GMB approximation.

3.1. Numerical results of the spectral function and DOS

Figure 1 presents plots of the spectral function $A(\boldsymbol{k}, \omega)\varepsilon_{\mathrm{F}}$ as a function of $\omega/\varepsilon_{\mathrm{F}}$ at $k = k_{\mathrm{F}}$. The values of $(k_{\mathrm{F}}a_{\mathrm{s}})^{-1}$ are (a) 0.2, (b) 0.01, (c) -0.2, (d) -0.4, and the corresponding transition temperatures $T_{\mathrm{c}}/T_{\mathrm{F}}$ are (a) 0.242, (b) 0.218, (c) 0.162, (d) 0.122. The two-peak structure persists up to $T = 1.02T_{\mathrm{c}}$ for $(k_{\mathrm{F}}a_{\mathrm{s}})^{-1} = 0.01$, $T = 1.03T_{\mathrm{c}}$ for $(k_{\mathrm{F}}a_{\mathrm{s}})^{-1} = -0.2$, and $T = 1.01T_{\mathrm{c}}$ for the $(k_{\mathrm{F}}a_{\mathrm{s}})^{-1} = -0.4$ case, and the definition of pseudogap is met when the temperature is slightly above T_{c}. We find the pseudogap persists up to $1.15T_{\mathrm{c}}$ for the $(k_{\mathrm{F}}a_{\mathrm{s}})^{-1} = 0.2$ case. The two-peak structure disappears with increasing temperature.

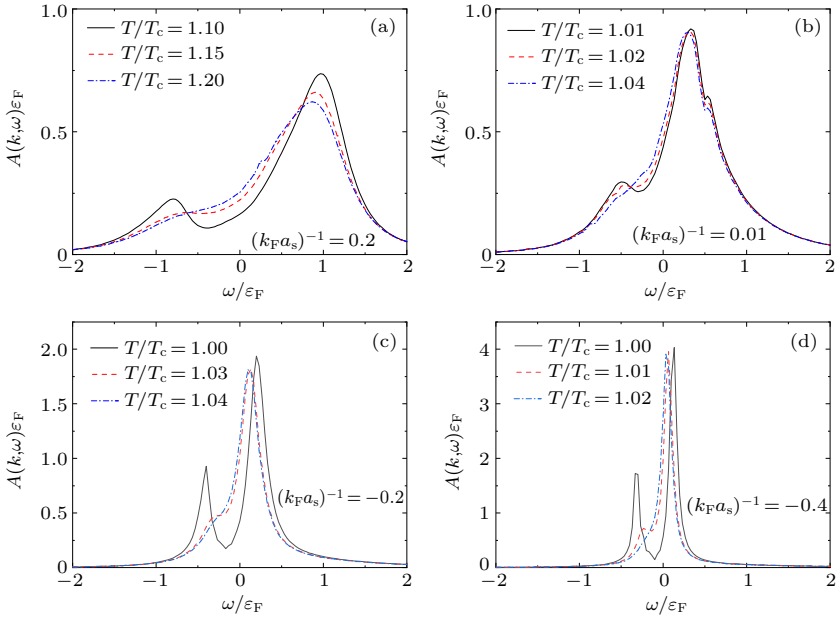


Fig. 1. Spectral function $A(\boldsymbol{k}, \omega)$ as a function of ω at $k = k_{\mathrm{F}}$ with GMB approximation. (a) $(k_{\mathrm{F}}a_{\mathrm{s}})^{-1} = 0.2$, (b) $(k_{\mathrm{F}}a_{\mathrm{s}})^{-1} = 0.01$, (c) $(k_{\mathrm{F}}a_{\mathrm{s}})^{-1} = -0.2$, (d) $(k_{\mathrm{F}}a_{\mathrm{s}})^{-1} = -0.4$.

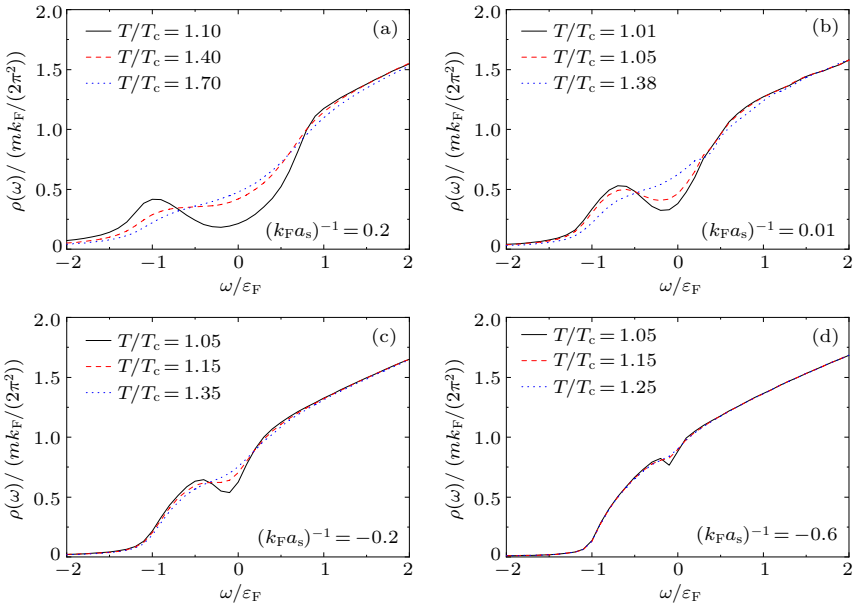


Fig. 2. Temperature dependence of density of states $\rho(\omega)$ with GMB approximation. (a) $(k_{\mathrm{F}}a_{\mathrm{s}})^{-1} = 0.2$, (b) $(k_{\mathrm{F}}a_{\mathrm{s}})^{-1} = 0.01$, (c) $(k_{\mathrm{F}}a_{\mathrm{s}})^{-1} = -0.2$, (d) $(k_{\mathrm{F}}a_{\mathrm{s}})^{-1} = -0.6$.

In Fig. 2, we show $\rho(\omega)/(mk_{\rm F}/(2\pi^2))$ as a function of $\omega/\varepsilon_{\rm F}$. The values of $(k_{\rm F}a_{\rm s})^{-1}$ are (a) 0.2, (b) 0.01, (c) -0.2, (d) -0.6. From Fig. 2, we find the pseudogap becomes more obvious with the increase of the value of $(k_{\rm F}a_{\rm s})^{-1}$. In each case, we plot the DOS at three different temperatures. We find a clear depletion at $T/T_{\rm c} = 1.05$ in the last three cases, but the depletion becomes obscure with increasing temperature. In the BEC side $(k_{\rm F}a_{\rm s})^{-1} = 0.2$, the depletion persists up to $1.7T_{\rm c}$. We determine the pseudogap temperature T^* where the depletion disappears. When $\mu < 0$, the GMB approximation is negligible with the disappearance of the Fermi surface. In this paper, we confine the discussion to the case of $\mu > 0$.

3.2. Pseudogap temperature

The numerical results of the pseudogap temperature as a function of $(k_{\rm F}a_{\rm s})^{-1}$ are plotted in Fig. 3. The black solid line is our result of the pseudogap temperature T^* from the DOS, and the red dashdot line corresponds to the pseudogap temperature T^{**} from the spectral function $A(\boldsymbol{k}, \omega)$. The pseudogap temperature monotonically increases with the increase of the strength of the pairing interaction. Although T^* and T^{**} are pseudogap temperatures, their values are different because one is associated with the spectral function, while the other is related to the momentum summation of the spectral function. One finds $T^* > T^{**}$.

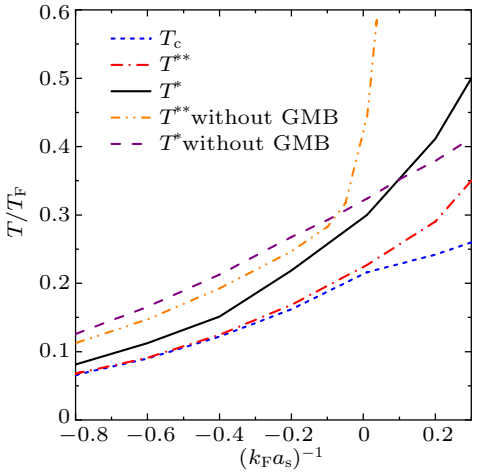


Fig. 3. Pseudogap temperature T^* and T^{**} as a function of $(k_{\rm F}a_{\rm s})^{-1}$. The black solid line is the pseudogap temperature T^* from DOS with GMB approximation. The red dashdot line corresponds to the pseudogap temperature T^{**} from the spectral function with particle–hole fluctuation. The blue short dashed line is the transition temperature $T_{\rm c}$ with GMB approximation. The theoretical calculations of pseudogap temperature T^* (the violet dashed line) and T^{**} (the orange dash-dot-dot line) without particle–hole fluctuation by Tsuchiya and co-workers from Ref. [26] are also plotted.

For comparison, theoretical calculations of the pseudogap temperature T^* (the violet dashed line) and T^{**} (the orange dash-dot-dot line) without particle–hole fluctuation by Tsuchiya and co-workers[26] are also plotted in Fig. 3. The pseudogap temperature T^{**} obtained by us is lower than the pseudogap temperature T^{**} by Tsuchiya and co-workers.[26] However, the situation is different for T^*. In the region $(k_{\rm F}a_{\rm s})^{-1} \lesssim 0.1$, our values are smaller than theirs; however, our results are larger when $(k_{\rm F}a_{\rm s})^{-1} > 0.1$. The transition temperature $T_{\rm c}$ (the blue short dashed line) calculated by us is also plotted in Fig. 3. From the figure, T^* is higher than $T_{\rm c}$, and the difference between them becomes bigger with increasing pairing interaction. The pseudogap temperature T^{**} is only slightly above $T_{\rm c}$ in the BCS side; however, the difference is growing in the BEC side.

At unitarity, according to our calculations, the pseudogap temperature T^* is $0.3T_{\rm F}$ and another pseudogap temperature T^{**} is $0.227T_{\rm F}$. We compare them with the experimental result reported in Ref. [18]. Pan and co-workers reported the pseudogap persisted up to the highest temperature $1.51T_{\rm c} \approx 0.257T_{\rm F}$. They also pointed out they estimated an onset pairing temperature $T \gtrsim 1.7T_{\rm c} \approx 0.29T_{\rm F}$. Our characteristic temperature T^{**} is lower than the experimental data; however, the pseudogap temperature T^* agrees well with the value they estimated.

4. Conclusion

In summary, we have investigated the pseudogap behavior of ultracold Fermi gases. We have computed the spectral function and DOS within the nTMA framework with the GMB approximation. From the DOS, we obtain the pseudogap temperature T^*. From the spectral function, we obtain another pseudogap temperature T^{**}. We compare the pseudogap temperatures T^* and T^{**} with the corresponding results without particle–hole fluctuation calculated by Tsuchiya and co-workers.[26] We find our pseudogap temperature T^{**} is always lower; however, the situation is different for T^*. We also compare our values with the experimental results in the unitary limit. We find pseudogap temperature T^* agrees well with the value they estimated in Ref. [18].

Acknowledgements

This work is supported by the National Laboratory of Solid State Microstructures of Nanjing University (Grant No. M37048), the Youth Talent Project of Anhui Education Department (Grant No. gxyq2019105), and the College Students Innovation and Entrepreneurship Training Program of Jiangsu University (Grant No. X2025102990894).

References

[1] Xiong L, Gong M, Fang Z X and Sun R 2023 *Chin. Phys. lett.* **40** 127402
[2] Ding P B, Shan B, Zhao Y H, Yang Y J, Chen L C, Meng Z M, Wang P J and Huang L H 2024 *Chin. Phys. B* **33** 063402
[3] Li Z L, Gu Z Y, Shi Z L, Wang P J and Zhang J 2023 *Chin. Phys. B* **32** 023701
[4] Giorgini S, Pitaevskii L P and Stringari S 2008 *Rev. Mod. Phys.* **80** 1215
[5] Bloch I, Dalibard J and Zwerger W 2008 *Rev. Mod. Phys.* **80** 885
[6] Chen Q J and Wang J B 2014 *Front. Phys.* **9** 539
[7] Mueller E J 2017 *Rep. Prog. Phys.* **80** 104401

[8] Hao J, Hong W, Zhou X, Xiang Y, Dai Y, Yang H, Li S, Luo H and Wen H H 2022 *Phys. Rev. B* **106** 014523
[9] Randeria M, Trivedi N, Moreo A and Scalettar R T 1992 *Phys. Rev. Lett.* **69** 2001
[10] Singer J M, Pedersen M H, Schneider T, Beck H and Matuttis H G 1996 *Phys. Rev. B* **54** 1286
[11] Jankó B, Maly J and Levin K 1997 *Phys. Rev. B* **56** R11407
[12] Yanase Y and Yamada K 2001 *J. Phys. Soc. Jpn.* **70** 1659
[13] Rohe D and Metzner W 2001 *Phys. Rev. B* **63** 224509
[14] Perali A, Pieri P, Strinati G C and Castellani C 2002 *Phys. Rev. B* **66** 024510
[15] Pines D 1997 *Z. Phys. B: Condens. Matter* **103** 129
[16] Kampf A and Schrieffer J R 1990 *Phys. Rev. B* **41** 6399
[17] Chakravarty S, Laughlin R B, Morr D K and Nayak C 2001 *Phys. Rev. B* **63** 094503
[18] Li X, Wang S, Luo X, Zhou Y Y, Xie K, Shen H C, Nie Y Z, Chen Q J, Hu H, Chen Y A, Yao X C and Pan J W 2024 *Nature* **626** 288
[19] Nozières P and Schmitt-Rink S 1985 *J. Low Temp. Phys.* **59** 195
[20] Gor'kov L P and Melik-Barkhudarov T K 1961 *Sov. Phys. JETP* **13** 1018
[21] Yu Z Q, Huang K and Yin L 2009 *Phys. Rev. A* **79** 053636
[22] Haussmann R 1993 *Z. Phys. B: Condens. Matter* **91** 291
[23] Haussmann R 1994 *Phys. Rev. B* **49** 12975
[24] Haussmann R, Rantner W, Cerrito S and Zwerger W 2007 *Phys. Rev. A* **75** 023610
[25] Chen Q J, Stajic J, Tan S N and Levin K 2005 *Phys. Rep.* **412** 1
[26] Tsuchiya S, Watanabe R and Ohashi Y 2009 *Phys. Rev. A* **80** 033613
[27] Pisani L, Perali A, Pieri P and Strinati G C 2018 *Phys. Rev. B* **97** 014528
[28] Strinati G C, Pieri P, Röpke G, Schuck P and Urban M 2018 *Phys. Rep.* **738** 1
[29] Strinati G C 2023 *Physica C* **614** 1354377
[30] Tajima H, Aoki H, Perali A and Bianconi A 2024 *Phys. Rev. B* **109** L140504
[31] Gong H, Ruan X X, Du L, Sun W M and Zong H S 2013 *Mod. Phys. Lett. B* **27** 1350214
[32] Ruan X X, Gong H, Du L, Sun W M and Zong H S 2013 *Phys. Rev. A* **87** 043608
[33] Ruan X X, Gong H, Du L, Jiang Y, Sun W M and Zong H S 2013 *Chin. Phys. Lett.* **30** 110303
[34] Ruan X X, Gong H, Wang Z L and Zong H S 2018 *Mod. Phys. Lett. B* **32** 1850249
[35] Ruan X X, Wang F, Gong H, Wang Z L and Zong H S 2018 *Mod. Phys. Lett. B* **32** 1850280